

## Body density affects stroke patterns in Baikal seals

Yuuki Watanabe<sup>1,\*</sup>, Eugene A. Baranov<sup>2,†</sup>, Katsufumi Sato<sup>3</sup>, Yasuhiko Naito<sup>4</sup> and Nobuyuki Miyazaki<sup>1</sup>

<sup>1</sup>*Ocean Research Institute, The University of Tokyo, 1-15-1 Minamidai, Nakano, Tokyo 164-8639, Japan,*

<sup>2</sup>*Limnological Institute, Siberian Division, Russian Academy of Sciences, Ulan-Batorskaya Street 3, Irkutsk 664033,*

*Russia, <sup>3</sup>International Coastal Research Center, Ocean Research Institute, The University of Tokyo, 2-106-1 Akahama, Otsuchi, Iwate 028-1102, Japan and <sup>4</sup>National Institute of Polar Research, 1-9-10, Kaga, Itabashi,*

*Tokyo 173-8515, Japan*

\*Author for correspondence (e-mail: yuuki@ori.u-tokyo.ac.jp)

†Present address: Baikal Seal Aquarium, 2nd Zheleznodorozhnaya Street 66, Irkutsk 664005, Russia

Accepted 22 June 2006

### Summary

Buoyancy is one of the primary external forces acting on air-breathing divers and it can affect their swimming energetics. Because the body composition of marine mammals (i.e. the relative amounts of lower-density lipid and higher-density lean tissue) varies individually and seasonally, their buoyancy also fluctuates widely, and individuals would be expected to adjust their stroke patterns during dives accordingly. To test this prediction, we attached acceleration data loggers to four free-ranging Baikal seals *Phoca sibirica* in Lake Baikal and monitored flipper stroking activity as well as swimming speed, depth and inclination of the body axis (pitch). In addition to the logger, one seal (Individual 4) was equipped with a lead weight that was jettisoned after a predetermined time period so that we had a set of observations on the same individual with different body densities. These four data sets revealed the general diving patterns of Baikal seals and also provided direct insights into the influence of buoyancy on these patterns. Seals repeatedly performed dives of a mean duration of 7.0 min (max. 15.4 min), interrupted by a mean surface duration of 1.2 min. Dive depths were 66 m on average, but varied substantially, with a maximum depth of 324 m. The seals showed

different stroke patterns among individuals; some seals stroked at lower rates during descent than ascent, while the others had higher stroke rates during descent than ascent. When the lead weight was detached from Individual 4, the seal increased its stroke rate in descent by shifting swimming mode from prolonged glides to more stroke-and-glide swimming, and decreased its stroke rate in ascent by shifting from continuous stroking to stroke-and-glide swimming. We conclude that seals adopt different stroke patterns according to their individual buoyancies. We also demonstrate that the terminal speed reached by Individual 4 during prolonged glide in descent depended on its total buoyancy and pitch, with higher speeds reached in the weighted condition and at steeper pitch. A simple physical model allowed us to estimate the body density of the seal from the speed and pitch (1027–1046 kg m<sup>-3</sup>, roughly corresponding to 32–41% lipid content, for the weighted condition; 1014–1022 kg m<sup>-3</sup>, 43–47% lipid content, for the unweighted condition).

Key words: buoyancy, diving, swimming, body composition, body density, data logger, Baikal seal, *Phoca sibirica*.

### Introduction

Buoyancy is one of the primary external forces acting on moving air-breathing divers, together with hydrodynamic drag and lift. The force is given as the difference between the total density of the body and that of the surrounding water:

$$B = (\rho_{\text{water}} - \rho_{\text{animal}})Vg, \quad (1)$$

where  $B$  is buoyancy in N,  $\rho_{\text{water}}$  and  $\rho_{\text{animal}}$  are the density (in kg m<sup>-3</sup>) of the surrounding water and the animal, respectively,  $V$  is the volume of the animal in m<sup>3</sup>, and  $g$  is the acceleration of gravity (=9.8 m s<sup>-2</sup>). The vertical force will be positive (i.e.

directed upward) if  $\rho_{\text{water}}$  is higher than  $\rho_{\text{animal}}$ , and negative if  $\rho_{\text{water}}$  is lower than  $\rho_{\text{animal}}$ . Animals that are positively or negatively buoyant must expend extra energy when they move in the direction opposite to this force, while they may save energy when moving in the same direction as this force. Consequently, buoyancy plays a significant role in the energy budget of diving birds (Stephenson et al., 1989; Lovvorn et al., 1991; Stephenson, 1994) and probably of other diving animals. Diving animals must therefore deal with buoyancy during the course of their daily diving activities.

To understand how and when free-ranging diving animals

work with or against buoyancy, it is necessary to monitor stroking activity of the animals during dives. This is now possible with the development of animal-borne accelerometers (Nowacek et al., 2001; Sato et al., 2002; Sato et al., 2003; van Dam et al., 2002; Watanuki et al., 2003; Watanuki et al., 2005; Watanuki et al., 2006; Lovvorn et al., 2004; Miller et al., 2004; Goldbogen et al., 2006; Kato et al., 2006), video cameras (Williams et al., 2000; Williams et al., 2004; Davis et al., 2001) and magnetic sensors (Wilson and Liebsch, 2002; Hays et al., 2004). These studies have shown that animals employ diverse stroke patterns across taxa according to their own buoyancy. Seals, for example, tend to adopt prolonged glides helped by negative buoyancy during descent, and ascend with more continuous stroking (Williams et al., 2000; Davis et al., 2001; Sato et al., 2003). On the other hand, diving birds (Sato et al., 2002; Wilson and Liebsch, 2002; Watanuki et al., 2003; Watanuki et al., 2005; Watanuki et al., 2006; Kato et al., 2006) and some whales (Nowacek et al., 2001; Miller et al., 2004) counteract positive buoyancy during descent by stroking, and use passive glides during ascent.

In marine mammals,  $\rho_{\text{animal}}$  is mainly determined by the relative amount of lipid and lean tissue since they have substantial amounts of blubber. While lean tissue is denser than water, lipid tissue is less dense, and animals with a large proportion of lipid will therefore have lower  $\rho_{\text{animal}}$  and be more buoyant (Webb et al., 1998; Beck et al., 2000; Biuw et al., 2003). The effect of air on  $\rho_{\text{animal}}$  should be minor in deep diving phocid seals, because, unlike fur seals (Hooker et al., 2005) and cetaceans (Ridgway et al., 1969), they are thought to exhale before diving (Falke et al., 1985). The effect of air on  $\rho_{\text{animal}}$  is also reduced by compression at depth (Biuw et al., 2003). Because  $\rho_{\text{animal}}$  can vary individually and seasonally as animals store energy in the form of lipid, this variability of  $\rho_{\text{animal}}$  would be expected to affect stroke patterns of individuals during dives. For instance, differences in stroke patterns across individuals were reported for Weddell seals *Leptonychotes weddellii* (Sato et al., 2003) and sperm whales *Physeter macrocephalus* (Miller et al., 2004). While Miller et al. had no information on fatness for each whale studied, Sato et al. reported that fatter seals (determined by the index calculated as axillary girth/standard length) predominantly showed stroke-and-glide swimming on descent, and that leaner seals were able to glide throughout most of this descent phase. However, the

effect of  $\rho_{\text{animal}}$  on inter-individual stroke patterns remains largely hypothetical because it was somewhat obscured in the previous work (Sato et al., 2003) by the fact that pitch (i.e. angle between long axis of animal's body and water surface) of some seals was restricted to less than 30° by the location of breathing holes in the ice and the slope of local bathymetric features. Buoyancy is a vertical vector and the magnitude of its component on the swimming direction is the magnitude of buoyancy weighted by  $\sin(\text{pitch})$ . The effect of buoyancy on stroke patterns should therefore be less evident at shallower pitch.

In this study, we conducted two experiments to test the hypothesis that  $\rho_{\text{animal}}$  affects stroke patterns in seals. In experiment 1, we attached acceleration data loggers to three Baikal seals *Phoca sibirica* to investigate the possible inter-individual variability of stroke patterns for the species. Lake Baikal was not covered by ice during the study periods, and the lake has a steep bathymetric slope in our study areas. Pitch of our seals was therefore not restricted by access to a breathing hole or by bathymetry. After validating the variability of stroke patterns among the individuals, we conducted experiment 2, where we attached a lead weight to one seal in addition to the acceleration logger. The weight was jettisoned after a predetermined time period so that for the same individual we had a set of observations of stroking activity under normal conditions (unweighted condition, lower  $\rho_{\text{animal}}$ ) and under artificially increased body density (weighted condition, higher  $\rho_{\text{animal}}$ ). If our hypothesis is correct, we would expect the seal to exhibit different stroke patterns between the two conditions; the seal in the weighted condition should adopt prolonged glides more readily in descent and stroke at higher rate in ascent, compared with the unweighted condition.

## Materials and methods

### Study site and animals

We conducted two types of experiments with a total of four Baikal seals *Phoca sibirica* Gmelin (Individuals 1–3 for experiment 1 and Individual 4 for experiment 2) in Lake Baikal, Russia, from 2002 to 2005. Table 1 gives descriptive information about the study animals. Individuals 1–3 were captured using modified twine gill-nets in autumn before the lake was frozen. Individual 4 was captured with nets put on

Table 1. Descriptive information for study animals

Experiment	Animal	Sex	Body mass (kg)	Capture		Release		Duration of captivity (months)
				Month/year	Location	Month/year	Location	
1	Individual 1	f	54.6	12/2002	Selenga River Delta, 52.5°N, 106.9°E	6/2003	Listvyanka, 51.9°N, 104.9°E	6
	Individual 2	f	72.8	12/2002	Selenga River Delta, 52.5°N, 106.9°E	6/2003	Listvyanka, 51.9°N, 104.9°E	6
	Individual 3	m	83.0	10/2004	Chivirkuy Bay, 53.9°N, 109.1°E	10/2004	Chivirkuy Bay, 53.9°N, 109.0°E	0
2	Individual 4	f	45.2	4/2005	Offshore in Middle Baikal, 52.7°N, 106.9°E	7/2005	Listvyanka, 51.9°N, 104.9°E	3

breathing holes on the ice in spring. Individuals 1, 2 and 4 were transported to the Limnological Institute Aquarium in Listvyanka after capture, and held in captivity before they were released on the shore in Listvyanka. Individual 3 was released at the site of capture without any period of captivity. Time-series diving data of Individuals 1 and 2 were reported earlier (Watanabe et al., 2004).

#### *Instruments*

To examine diving behavior of the seals, we used two types of multi-sensor data loggers: UWE1000-PD2GT (22 mm in diameter, 124 mm in length, 92 g in air; Little Leonardo Co., Tokyo, Japan) and W1000L-3MPD3GT (26 mm in diameter, 175 mm in length, 135 g in air; Little Leonardo Co.). PD2GT was used for Individuals 1 and 2 (experiment 1) to record swimming speed, depth and temperature at 1 s intervals, and 2-D accelerations (for detecting flipper movement and pitch) at 1/16 s intervals, with a memory of 32 Mb. 3MPD3GT was used for Individual 3 (experiment 1) and Individual 4 (experiment 2) to record swimming speed, depth, temperature and 3-D geomagnetism at 1 s intervals, with a memory of 512 Mb. 3-D accelerations were also recorded at 1/16 s and 1/32 s intervals for Individual 3 and 4, respectively. The maximum range of the depth sensor was 1000 m with a resolution of 0.24 m for all instruments. In addition to the multi-sensor loggers, we attached a digital still-picture logger (DSL-380DTV: 22 mm in diameter, 138 mm in length, 73 g in air; Little Leonardo Co.) to each seal. Because this study was focused on stroke patterns of the seals, we did not use geomagnetic data obtained from the 3MPD3GT or still picture data recorded by the DSL.

The total weight of the instruments deployed on Individuals 1 and 2, including devices for data recovery (such as float and VHF transmitter; see below), was 360 g in air and its buoyancy offset 110 g in water. The system used for Individuals 3 and 4 weighed 370 g in air and its buoyancy offset 85 g in water. Additional drag due to the instrument is considered in Discussion.

In experiment 2, we deployed a lead weight in the shape of a flat plate with rounded corners (10 cm long  $\times$  9 cm wide  $\times$  1.5 cm deep, 1.45 kg in air) just behind the loggers on the seal's back. The weight was automatically detached 24 h after deployment by a time-scheduled release mechanism (Little Leonardo Co.; see below), while the loggers were released from the animal after 72 h for data recovery.

#### *Data recovery*

Our animal-borne data loggers require physical recovery for data retrieval but the recapture of instrumented Baikal seals in Lake Baikal is almost impossible (Baranov, 1996). We therefore used an automatic time-scheduled release system (Watanabe et al., 2004) that allows the loggers to be located and retrieved using VHF radio signals. Recapture of seals is therefore not necessary. The data loggers were attached to a float of copolymer foam (Nichiyu Giken Kogyo Co., Saitama, Japan), in the top of which a VHF radio transmitter with a 45 cm semi-rigid wire antenna (Advanced Telemetry Systems

Inc., Isanti, MN, USA) was embedded [see fig. 1 in (Watanabe et al., 2004)]. A plastic cable connected to a time-scheduled release mechanism (Little Leonardo Co.) bound the package to an aluminum plate, which was glued onto the seals with a quick-setting epoxy resin (ITW Devcon Co., Osaka, Japan). The release mechanism included a timer that was activated 24 h and 72 h after attachment for experiment 1 and 2, respectively. Once the release mechanism had been activated, the plastic cable was severed by an electric charge from the battery of the device, and the whole buoyant package was released from the seal. Once the package had floated to the surface of the lake it could be located *via* VHF radio-signals using a receiver and a 4-element Yagi antenna (Ham Center Sapporo Co., Hokkaido, Japan). A reward was offered for the return of the package to facilitate recovery in case we failed to locate it. The same release mechanism was used to detach the lead weight from the seal after 24 h in experiment 2.

The packages were successfully retrieved using VHF radio signals on all three attempts in experiment 1. However, on the attempt in experiment 2, we were not able to catch VHF radio signals from the package and failed to recover it by ourselves. Fortunately, it was found by a tourist and sent to us 2 weeks after its release from the seal.

#### *Depth data analysis*

Based on the sensor's absolute accuracy, a dive was defined as any excursion below the surface to a depth of  $>2$  m. To examine the stroke pattern of the seals while descending and ascending, each dive was subdivided into a descent phase (from the beginning of a dive to the time of the first ascent), an ascent phase (from the time of the last descent to the end of the dive), and a bottom phase (the time between the end of descent and beginning of ascent). The expression 'dive depth' hereafter refers to the maximum depth reached during a dive.

#### *Acceleration data analysis*

The PD2GT and 3MPD3GT loggers use 2-axis (sway and surge) and 3-axis (sway, surge and heave) acceleration sensors, respectively, that measure both dynamic acceleration (such as propulsive activities) and static acceleration (such as gravity or pitch).

Swaying accelerations often contained low frequency variations that were assumed to be the result of various turning and rolling movements by the seals. These were separated using the highpass filter function of the software application IGOR Pro (WaveMetrics Inc., Lake Oswego, OR, USA) to extract the information on flipper stroking activity. To select an appropriate filter band, we calculated the power spectral density of each swaying acceleration record using a Fast Fourier Transformation with IGOR Pro. This calculation showed a clear trough between two peaks at 0 Hz and each seal's dominant stroke frequency (0.6–1.3 Hz). The trough bands (0.75, 0.69, 0.44 and 0.75 Hz for Individuals 1, 2, 3 and 4, respectively) were used for filtering. The filtered accelerations were then smoothed using IGOR Pro (binomial smoothing, 10 passes) to remove noise at frequencies above the

stroke rate, and the remaining peaks and troughs with absolute amplitudes greater than a set threshold were considered to represent individual strokes (Sato et al., 2003). The threshold was determined for each individual (0.2, 0.4, 0.3 and 0.5 m s<sup>-2</sup> for Individuals 1, 2, 3 and 4, respectively) after visual inspection. Both a peak and a trough correspond to a single flipper stroke (i.e. left-to-right or right-to-left). Flipper stroke rate (s<sup>-1</sup>) during descent and ascent was calculated from the total number of strokes divided by the duration of each phase (ascent and descent) for each dive.

When a seal is still or moving at a constant speed, surging accelerations will change with the component of gravity along the body axis of the seal, allowing pitch to be calculated. However, surging accelerations are also affected by flipper driven forward movements (Tanaka et al., 2001; Yoda et al., 2001). High-frequency variations in the surging acceleration record are believed to be caused by flipper movements, and are therefore associated with forward movements (Sato et al., 2003). By filtering out these high-frequency signals from the surging acceleration using a low-pass filter (IGOR Pro), with the same threshold as that used for swaying accelerations, the animal's pitch was calculated. Descents are represented as negative pitch while ascents are indicated by positive pitch values.

#### Speed calibration

Relative swimming speed through water was recorded as the number of rotations per second (rev s<sup>-1</sup>) of an external propeller mounted at the anterior end of the loggers. The rotation value was converted to actual swimming speed (m s<sup>-1</sup>) using the calibration method (Sato et al., 2003). Briefly, we plotted propeller rotations (rev s<sup>-1</sup>) against the speed calculated from depth change and pitch ( $U_{cal}=U_{ver}/\sin|\theta|$ ) for each second, where  $U_{ver}$  is vertical speed determined from the depth recorder and  $\theta$  is pitch of the seal. Then we used linear least-squares regression to obtain swimming speed from a given propeller rotation. This method is more reliable for steeper pitch, and hence we used only  $\sin|\theta|>0.9$  in our calculations. Correlation coefficients were 0.959, 0.958, 0.890 and 0.950 with  $N$  of 15479, 9592, 40881 and 34472 for Individuals 1, 2, 3 and 4, respectively. Resolutions of swimming speed, which correspond to one rotation of the propeller, were 0.069, 0.066, 0.020 and 0.019 m s<sup>-1</sup> for Individuals 1, 2, 3 and 4, respectively. Rotation values of rev s<sup>-1</sup> were not converted to swimming speed when they were lower than the stall rev s<sup>-1</sup> of the logger, determined experimentally to be 0.3 m s<sup>-1</sup>.

#### Selection of dives for stroke pattern analysis

After reporting general dive variables (i.e. dive depth, dive duration and surface duration), we selected dives for further analysis and examined the effect of buoyancy on stroke patterns, according to the following two criteria. (1) Mean absolute value of pitch in descent and ascent should be  $>30^\circ$ . At this pitch, the magnitude of the component of buoyancy vector along the swimming direction is the magnitude of

buoyancy weighted by more than  $\sin(30^\circ)=0.5$ , and the effects of the force on stroke patterns should therefore be more evident. (2) The depth at both the end of descent and start of ascent should be  $>15$  m, because stroke rate in descent or ascent is not reliable for dives with very short descent or ascent phases.

#### Calculation of drag coefficient

Besides buoyancy, mobile aquatic organisms are affected by drag. Because the objective of experiment 2 was to investigate the possible effect of body density, or buoyancy, on stroke patterns, it is important to know whether drag differed between the weighted and the unweighted conditions. This was achieved by calculating drag coefficients from deceleration rates during horizontal glides (Clark and Bemis, 1979; Bilo and Nachtigall, 1980; Videler and Kamermans, 1985; Williams and Kooyman, 1985; Feldkamp, 1987; Stelle et al., 2000; Ribak et al., 2005).

We randomly extracted a total of 200 deceleration phases (100 for each condition) from the periods when the seal swam horizontally (determined from the depth recorder) using the stroke-and-glide method during the bottom phases of dives (Fig. 1). Drag ( $D$ ) in N was calculated from deceleration rate as:

$$D = m_{\text{seal}}m_e(U_t - U_{t+1}), \quad (2)$$

where  $m_{\text{seal}}$  is mass of Individual 4 for the weighted (46.65 kg) and unweighted (45.2 kg) condition, respectively, and  $m_e$  is a multiplier for entrained water attached to the surface of the seal (total mass= $m_{\text{seal}}m_e$ ). The value for  $m_e$  was set to 1.06 based on the measure for a prolate spheroid of fineness ratio 5.0 (Skrovan et al., 1999; Miller et al., 2004).  $U_t$  and  $U_{t+1}$  are swimming speeds (m s<sup>-1</sup>), with a resolution of 0.019 m s<sup>-1</sup>, at  $t$  and  $t+1$  (s), respectively, and were averaged to describe the mean glide speed ( $U$ ). Drag coefficient ( $C_d$ ), based on frontal area, was then given by:

$$C_d = 2D / (\rho_{\text{water}}A_fU^2), \quad (3)$$

where  $\rho_{\text{water}}$  is water density (1000 kg m<sup>-3</sup>; note that Baikal

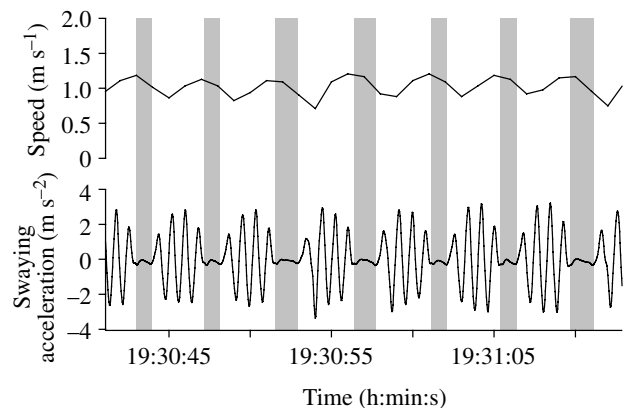


Fig. 1. Speed and swaying acceleration during stroke-and-glide swimming. Grey vertical bars denote periods of glide. Deceleration rates during glides were used to calculate drag. The experiment was conducted on July 6, 2005.

seals are freshwater seals).  $A_f$  is the frontal area of the seal ( $0.0911 \text{ m}^2$ ) calculated from the girth measurement, assuming that seals are circular in cross section.  $C_d$  is reported with Reynolds number ( $Re$ )= $LU/\nu$ , where  $L$  is total length of the seal (1.24 m) and  $\nu$  is kinematic viscosity of freshwater at the mean water temperature of  $5^\circ\text{C}$  measured by the logger [ $1.520 \times 10^{-6} \text{ m}^2 \text{ s}^{-1}$  (Anon, 2004)].

Cormorants swim at shallow depth in a tank with their body angled to the swimming direction to counter positive buoyancy, and the tilt of the body increases the drag coefficients (Ribak et al., 2005). In this study, we assumed that seals have no ‘angle of attack’ during horizontal glides. Though this assumption might not be entirely correct, the effect should be small because the seal was probably close to neutral buoyancy at the depths where we extracted horizontal glides (Weighted,  $23.7 \pm 6.3 \text{ m}$ ; Unweighted,  $36.1 \pm 5.8 \text{ m}$ ).

#### Terminal speed and body density

An object sinking through water with negative buoyancy will eventually reach its terminal speed (i.e. the speed at which drag equals the magnitude of the negative buoyancy), which depends on the density of the object. We tested if seals reached their terminal speeds during prolonged glide in descents, to determine if the body density of seals could be calculated from the measured speed.

Consider a seal with a body density of  $\rho_{\text{seal}}$  descending by prolonged glide at a pitch of  $\theta$ . At the theoretical terminal speed ( $U_{\text{ter}}$ ), drag equals the magnitude of negative buoyancy weighted by  $\sin|\theta|$ :

$$0.5C_d\rho_{\text{water}}A_fU_{\text{ter}}^2 = (1-\rho_{\text{water}}/\rho_{\text{seal}})mgsin|\theta|. \quad (4)$$

The equation represents the relationship between two unknown variables,  $U_{\text{ter}}$  and  $\rho_{\text{seal}}$ . A model simulation was conducted under several theoretically possible values of  $\rho_{\text{seal}}$  ( $1000\text{--}1050 \text{ kg m}^{-3}$ ) with a variable of  $\theta$  measured every second. The simulated speeds were then compared with the measured speed. If a simulation run with an appropriate value of  $\rho_{\text{seal}}$ , determined by least-squares method, gave a  $U_{\text{ter}}$  that fit with speed measured during the course of the prolonged glide, then we knew the seals were at terminal speed for that measured speed. We could then use the measured speed (as  $U_{\text{ter}}$ ) and  $\theta$  to calculate the seal’s actual  $\rho_{\text{seal}}$  for each glide. Residual air in the lung will have a significant influence on our predictions of  $\rho_{\text{animal}}$ , but this bias is substantially reduced at greater depths because of the exponential decrease in air volume with increasing depth (Biuw et al., 2003). We therefore excluded speeds and pitches measured at depths  $<100 \text{ m}$  from our calculations. Strictly speaking, gliding seals should generate lift to maintain  $\theta$ , and induced drag, the consequence of producing lift (Vogel, 1994), should be included on the left in Eqn 4. However, we were not able to include it due to lack of information on how these seals produce lift. The consequence of this simplification is considered in ‘Discussion’.

#### Statistical analysis

Statistical analysis was performed using Stat View (SAS

Institute Inc., Cary, NC, USA). Values for statistical significance were set at  $P<0.05$ . Means ( $\pm$  s.d.) are reported.

## Results

Recording periods for Individuals 1, 2, 3 (experiment 1) and 4 (experiment 2) lasted 20, 20, 24 and 72 h, respectively, providing a total of 178, 160, 116 and 489 dives, respectively. Because these four data sets are the first time-series records of the diving behavior of Baikal seals, we report dive depth, dive duration and surface duration in more detail than might normally be presented (Table 2). Over all of the dives ( $N=740$ ), excluding those under the weighted condition in experiment 2, the mean and maximum dive depths were  $66.1 \pm 53.7 \text{ m}$  and  $324 \text{ m}$ , respectively, and mean and maximum durations were  $7.0 \pm 2.6 \text{ min}$  and  $15.4 \text{ min}$ , respectively.

The number of dives meeting the depth and pitch selection criteria for stroke pattern analysis was 104, 70, 94 for Individual 1, 2 and 3, respectively, in experiment 1. The seals demonstrated different patterns in terms of stroke rate in descent and ascent (Figs 2, 3). Individuals 1 and 3 had significantly lower stroke rates in descent (Individual 1,  $1.45 \pm 0.45 \text{ s}^{-1}$ ; Individual 3,  $0.26 \pm 0.16 \text{ s}^{-1}$ ) than ascent (Individual 1,  $1.82 \pm 0.18 \text{ s}^{-1}$ ; Individual 3,  $1.03 \pm 0.28 \text{ s}^{-1}$ ; Wilcoxon test,  $P<0.0001$  for Individuals 1 and 3), while Individual 2 had significantly higher stroke rate in descent ( $1.81 \pm 0.29 \text{ s}^{-1}$ ) than ascent ( $1.20 \pm 0.28 \text{ s}^{-1}$ ; Wilcoxon test,  $P<0.0001$ ). Individual 3 glided throughout most of the descent phases, resulting in remarkably low stroke rate in descent.

In experiment 2, Individual 4 was in the weighted condition for the first 24 h until the weight was jettisoned, after which the unweighted condition lasted 48 h. There were no significant differences in dive depths between the weighted ( $62.9 \pm 49.0 \text{ m}$ ,  $N=177$  dives) and unweighted ( $58.9 \pm 54.6 \text{ m}$ ,  $N=311$  dives) conditions (Mann–Whitney  $U$ -test,  $P=0.95$ ), while dive duration was significantly shorter for the weighted ( $5.8 \pm 2.5 \text{ min}$ ,  $N=177$  dives) than unweighted ( $7.5 \pm 2.0 \text{ min}$ ,  $N=311$  dives) condition (Mann–Whitney  $U$ -test,  $P<0.0001$ ).

Drag, calculated from deceleration rates during horizontal glides, and mean glide speed ranged from  $1.0$  to  $9.4 \text{ N}$  and from  $0.57$  to  $1.35 \text{ m s}^{-1}$  ( $N=100$ ), respectively, for the weighted condition, and from  $1.4$  to  $8.1 \text{ N}$  and from  $0.60$  to  $1.27 \text{ m s}^{-1}$  ( $N=100$ ), respectively, for the unweighted condition. There was no significant difference in drag coefficient based on frontal area between the weighted ( $0.11 \pm 0.029$  at  $Re$  of  $8.7 \pm 1.3 \times 10^5$ ) and unweighted ( $0.11 \pm 0.019$  at  $Re$  of  $8.8 \pm 1.0 \times 10^5$ ) condition (Mann–Whitney  $U$ -test,  $P=0.55$ ). We used a  $C_d$  value of  $0.11$  for calculation of terminal speed and body density (Eqn 4).

The number of dives meeting the depth and pitch selection criteria for stroke pattern analysis was 73 and 109 for the weighted and unweighted condition, respectively, in experiment 2. Examples of stroke patterns of the seal weighted and unweighted are shown in Fig. 4. Descent stroke rate was significantly lower for the weighted ( $0.26 \pm 0.23 \text{ s}^{-1}$ ) than unweighted ( $0.93 \pm 0.36 \text{ s}^{-1}$ ) condition (Mann–Whitney  $U$ -test,  $P<0.0001$ ). Ascent stroke rate was significantly higher for the

Table 2. Summary of diving behavior of Baikal seals

	Individual 1	Individual 2	Individual 3	Individual 4 <sup>a</sup>	All data
Data length (h)	20	20	24	48	112
No. of dives	164	151	114	311	740
Dive depth (m)					
Mean	72.3	65.2	77.7	58.9	66.1
s.d.	57.4	48.4	49.4	54.6	53.7
Median	58.0	53.7	66.2	41.6	51.1
Maximum	234.2	242.1	222.3	324.0	324.0
Dive duration (min)					
Mean	5.7	6.4	8.1	7.5	7.0
s.d.	2.8	2.8	2.7	2.0	2.6
Median	5.7	6.4	7.9	7.4	7.2
Maximum	11.2	13.5	15.4	14.4	15.4
Surface duration (min) <sup>b</sup>					
Mean	1.3	1.4	1.3	1.1	1.2
s.d.	0.6	0.5	0.6	0.3	0.5
Median	1.3	1.3	1.2	1.0	1.2
Maximum	4.2	2.8	5.4	2.2	5.4

<sup>a</sup>Data in the weighted condition were excluded.

<sup>b</sup>Surface durations between bouts (>14 min; 2, 3 and 3 surfacings for Individuals 1, 3 and 4, respectively) were excluded.

weighted ( $2.36 \pm 0.11 \text{ s}^{-1}$ ) than unweighted ( $1.53 \pm 0.19 \text{ s}^{-1}$ ) condition (Mann–Whitney *U*-test,  $P < 0.0001$ ; Fig. 3).

We categorized the diving behavior of Individual 4 during descent and ascent phases into three swimming modes based on stroking patterns and swimming speed: prolonged glide, stroke-and-glide and continuous stroking (Sato et al., 2003). Prolonged glides were characterized by periods with no flipper movement, and an initial increase of swimming speed that gradually leveled off (Fig. 4A,C,D). Stroke-and-glide behavior was defined by intermittent strokes and corresponding fluctuations in swimming speed (Fig. 4B,D). During continuous stroking, swimming speed remained relatively constant (Fig. 4A,C).

Two patterns of swimming mode usage were observed during descent: in some dives, the seal adopted stroke-and-glide throughout the descent (Fig. 4B), while in other dives, stroke-and-glide was employed at the beginning of the descent but a prolonged glide was adopted for the remainder of the descent (Fig. 4A,C,D). The latter pattern will be referred to as merely 'prolonged glide' in this paragraph. In prolonged glides, glide phases started at significantly shallower depths in the weighted ( $9.9 \pm 4.0 \text{ m}$ ,  $N=70$  dives) than the unweighted ( $49.8 \pm 17.0 \text{ m}$ ,  $N=36$  dives) condition (Mann–Whitney *U*-test,  $P < 0.0001$ ). We grouped dives into 50 m bins based on dive depths to show the occurrence of stroke-and-glide and prolonged glides during descent (Fig. 5). In the weighted condition, the seal adopted prolonged glide significantly more frequently than the unweighted condition in dives of <150 m ( $\chi^2$  test;  $P < 0.0001$  for 0–50 m and 50–100 m,  $P < 0.005$  for 100–150 m). In dives of 150–200 m, the seal adopted prolonged glide in all dives in the weighted condition and in

most of dives (5 out of 6) in the unweighted condition, and the difference was not statistically significant ( $\chi^2$  test,  $P=0.095$ ). In dives of >200 m, the seal always adopted prolonged glide, regardless of whether it was in the weighted or unweighted condition. When ascending, the seal adopted either stroke-and-glide (Fig. 4B,D) or continuous stroking (Fig. 4A,C) throughout the period. In the weighted condition, the seal adopted continuous stroking in a significantly higher proportion of dives than in the unweighted condition in all depth bins except 200–250 m and 300–350 m, where no dives were recorded in the weighted condition ( $\chi^2$  test;  $P < 0.0001$  for 0–50 m, 50–100 m and 100–150 m,  $P < 0.01$  for 250–300 m; Fig. 5).

After the start of the prolonged glide, the measured speed increased to reach a first peak under both conditions (Fig. 6). When an appropriate value of body density was used, the theoretical terminal speed fit well with the measured speed in the portion after the peak. In other words, once the seal reached the peak in speed, the change in speed was well explained by the change in pitch. For the examples in Fig. 6, theoretical terminal speeds that fit well with the measured speeds were obtained using body densities of  $1043 \text{ kg m}^{-3}$  and  $1015 \text{ kg m}^{-3}$  for the weighted and unweighted condition, respectively.

Fig. 7 shows the relationship between maximum speed in each prolonged glide measured at the depth of >100 m, and pitch at the moment when the speed was recorded. Theoretical terminal speeds for several body densities are also shown. The speeds were higher for the weighted than the unweighted condition at all pitches. There were significant negative relationships between the speed and pitch for both the weighted (Spearman  $R = -0.965$ ,  $N=28$ ,  $P < 0.0001$ ) and unweighted

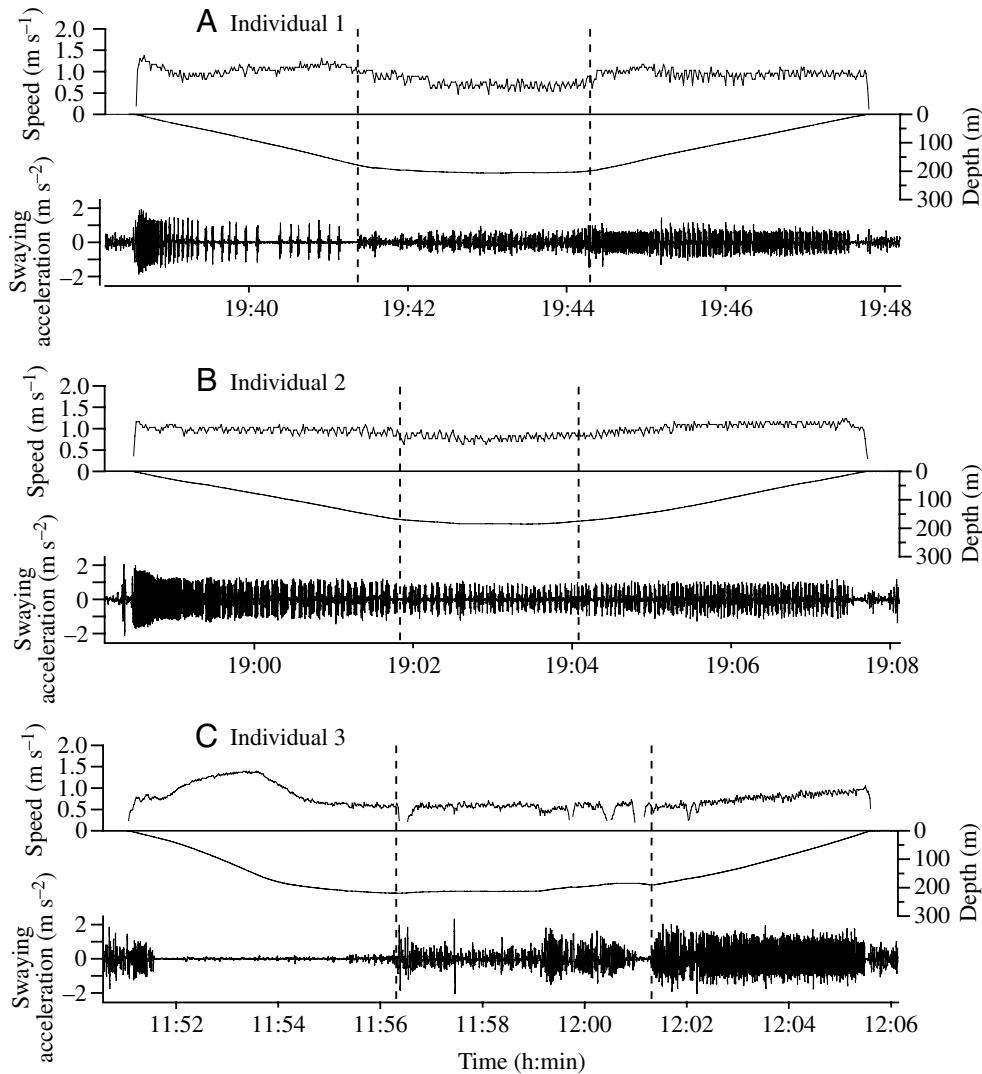


Fig. 2. Typical dives made by (A) Individual 1 (June 19, 2003), (B) Individual 2 (June 22, 2003) and (C) Individual 3 (November 1, 2004), showing swimming speed, depth and swaying acceleration. Vertical broken lines separate dives into three phases: descent, bottom and ascent. Note that stroke patterns in descent and ascent differ among the individuals.

(Spearman  $R = -0.782$ ,  $N = 25$ ,  $P < 0.0005$ ) conditions (i.e. speed is higher at steeper pitch since pitch is negative when descending). The body densities calculated from the speeds and pitches using Eqn 4 ranged from 1027 to 1046  $\text{kg m}^{-3}$  ( $N = 28$  glides) for the weighted condition, and from 1014 to 1022  $\text{kg m}^{-3}$  ( $N = 25$  glides) for the unweighted condition.

## Discussion

### *Diving behavior of Baikal seals*

The Baikal seal is one of the few phocid species in which free-ranging diving behavior remains relatively unknown. In previous research, satellite-linked transmitters were deployed on four juvenile Baikal seals to obtain histograms of dive depth and duration, composed of six bins for each parameter (Stewart et al., 1996). The most frequent dive depth and duration bins were 10–50 m and 2–6 min, respectively. In our earlier work (Watanabe et al., 2004), we reported time-series diving data on two Baikal seals (Individuals 1 and 2). In the present study, we added two more data sets and presented variables representing

the diving capability of Baikal seals. They repeatedly performed dives of a mean duration of 7.0 min (max. 15.4 min), interrupted by a mean surface duration of 1.2 min. Dive depths were 66 m on average, but varied substantially, with maximum depth of 324 m. The dive depth of 324 m is the current record for Baikal seals.

Dive durations are especially important since Baikal and Weddell seals are the two phocid species for which the aerobic dive limit [ADL, i.e. the dive duration beyond which metabolism becomes anaerobic and post-dive lactate concentration increases above the resting level (Kooyman, 1985)], has been directly measured [Baikal seals (Ponganis et al., 1997); Weddell seals (Kooyman et al., 1980; Kooyman et al., 1983; Burns and Castellini, 1996)]. The measured ADL of Baikal seals is 15 min, and only two of the total 740 dives (0.3%) in this study exceeded that. This supports the conclusion from Weddell seal studies that even long-duration and deep-diving phocids rely on aerobic metabolism in the great majority of the diving time (for a review, see Kooyman and Ponganis, 1998). However, it should be noted that

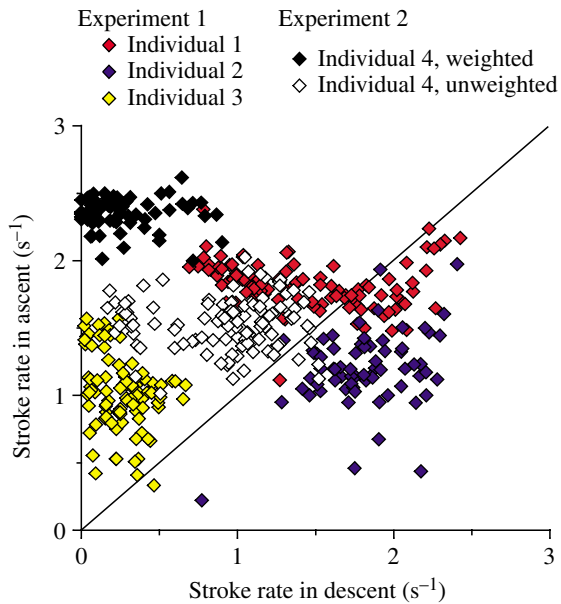


Fig. 3. Relationship between stroke rate in descent and ascent for Individuals 1–3 in experiment 1 and Individual 4 in experiment 2. The diagonal line represents identical stroke rate in both directions.

Ponganis et al. measured plasma lactate concentrations of Baikal seals after the animals had been submerged in a 3 m-deep tank rather than after dives in Lake Baikal (Ponganis et al., 1997). Submersion in the tank should be less costly than dives in the lake and hence the ADL measured by Ponganis et al. of 15 min is probably longer than for seals diving in the lake under natural conditions.

#### Stroke patterns

In experiment 1, we showed that Baikal seals used variable stroke patterns across individuals in terms of stroke rate in descent and ascent; Individuals 1 and 3 had lower stroke rates in descent than ascent while Individual 2 had higher stroke rates in descent than ascent (Fig. 3). A similar result was reported for sperm whales; some individuals stroked more in descent than ascent but others stroked less in descent than ascent (Miller et al., 2004). Intra-specific variabilities of stroke patterns were also reported for Weddell seals (Sato et al., 2003). They suggest that the patterns were affected by the relative fatness of the seals: thinner animals having lower stroke rates in descent than ascent and fatter ones having higher stroke rates in descent than ascent. Our second experiment using a lead weight with a jettison system provides direct evidence that body density (which in phocids is largely a function of the relative proportions of lean and lipid tissue) affects stroke patterns in seals. In experiment 2, we showed that the seal changed its stroke pattern when the lead weight was detached; stroke rate in descent increased and that in ascent decreased (Fig. 3). Given that having the lead weight simulates a reduction in fatness by increasing the total body density, the observed changes in stroke rate due to the

jettison of the weight are consistent with the relationship between stroke patterns and fatness in Weddell seals (Sato et al., 2003). Unlike Sato et al., we examined the difference in stroke patterns within an individual by artificially altering its body density, hence avoiding any confounding effects caused by differences in body size or other individual characteristics.

It is important to point out that the change in stroke rate arose mainly from a change in swimming modes. While in the weighted condition, the seal adopted prolonged glide during descent and continuous strokes during ascent. While in the unweighted condition, the seal used stroke-and-glide swimming throughout its descent and ascent, except for deeper dives (>150 m) where it adopted prolonged glide during descent (Figs 4, 5). In the descent phases where prolonged glides were observed, the seal in the weighted condition began gliding at shallower depths than in the unweighted condition, demonstrating that seals are able to use prolonged glide below a particular depth depending upon individual body densities. Below these depths, ambient pressure probably compresses the residual gas in the lungs sufficiently to make the seals negatively buoyant (Skrovan et al., 1999; Williams et al., 2000).

It is possible that additional drag due to the lead weight could affect stroke patterns of the seal in the weighted condition. This is unlikely to have contributed to the observed changes, however, since there was no significant difference in drag coefficient between the weighted and the unweighted condition. Extra drag caused by the weight should be minimal because the flat-shaped weight was attached just behind the logger package on the seal's back so that the frontal area did not differ between the two conditions.

#### The effect of the lead weight on body density

How much did the lead weight of 1.45 kg alter the body density of the seal in experiment 2? The difference in body density of the seal between the weighted and the unweighted condition ( $\Delta\rho$ ) is:

$$\Delta\rho = \frac{m_{\text{seal}} + m_{\text{weight}}}{\left(\frac{m_{\text{seal}}}{\rho_{\text{seal}}} + \frac{m_{\text{weight}}}{\rho_{\text{weight}}}\right)} - \rho_{\text{seal}}, \quad (5)$$

where  $m_{\text{seal}}$  and  $m_{\text{weight}}$  are the mass of the seal (45.2 kg) and the lead weight (1.45 kg), respectively,  $\rho_{\text{seal}}$  and  $\rho_{\text{weight}}$  are the density of the seal and the weight ( $11350 \text{ kg m}^{-3}$ ), respectively. Although  $\rho_{\text{seal}}$  is unknown,  $\Delta\rho$  is insensitive to  $\rho_{\text{seal}}$ ; the possible range of  $\rho_{\text{seal}}$  ( $1000\text{--}1050 \text{ kg m}^{-3}$ ) gives the narrow range of  $\Delta\rho$  ( $29.2\text{--}30.5 \text{ kg m}^{-3}$ ). This shows that the lead weight should increase the body density of the seal by  $\sim 30 \text{ kg m}^{-3}$ .

To provide an idea what this change corresponds to in terms of the relative amount of lipid, consider the following scenario. The total density of the seal ( $\rho_{\text{seal}}$ ) is calculated as:

$$\rho_{\text{seal}} = \rho_{\text{lipid}}P_{\text{lipid}} + \rho_{\text{lipid-free}}(1-P_{\text{lipid}}), \quad (6)$$

where  $\rho_{\text{lipid}}$  and  $\rho_{\text{lipid-free}}$  are the density of body lipid and lipid-free-body of seals, respectively.  $P_{\text{lipid}}$  is the proportion of body



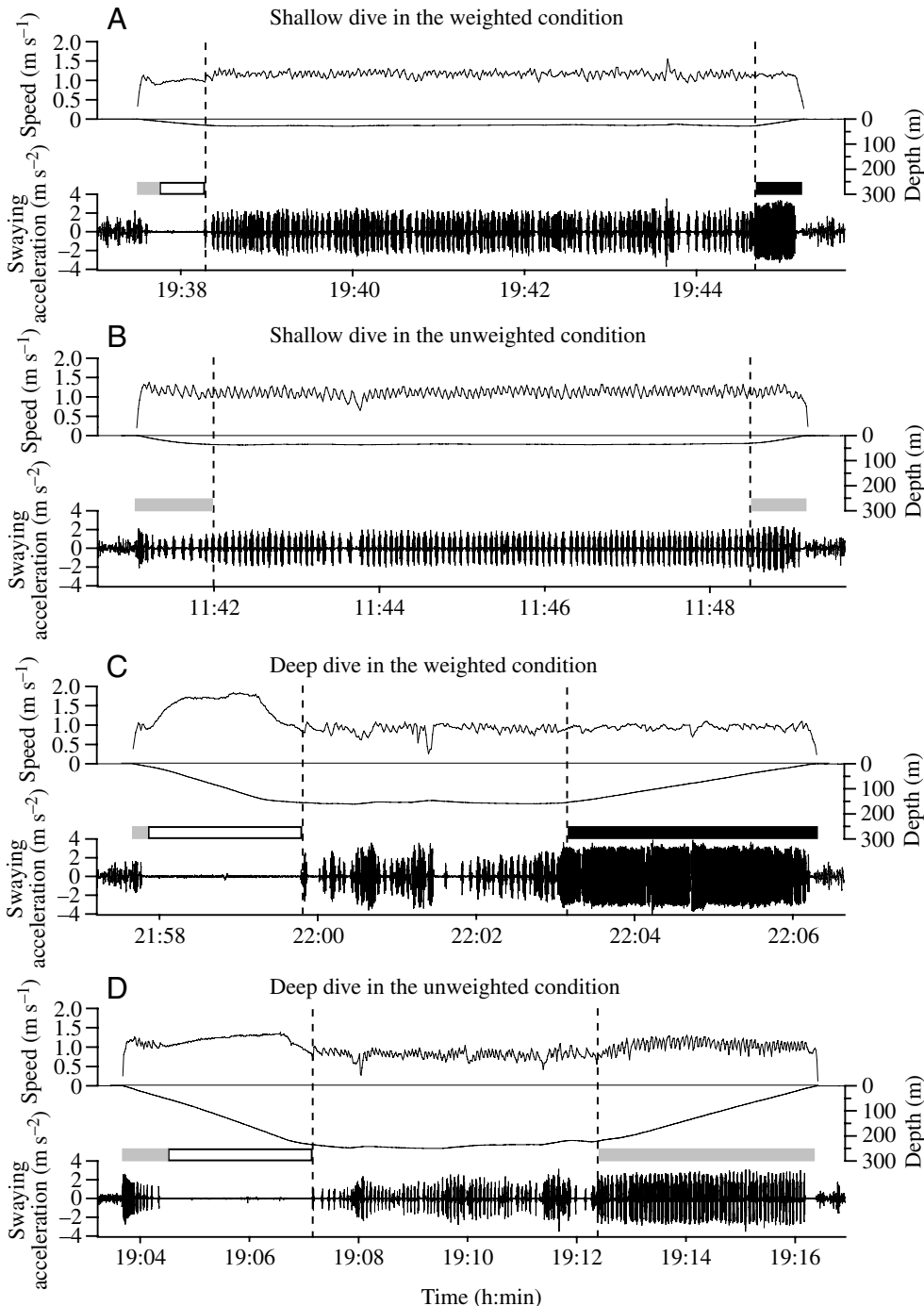


Fig. 4. Swimming speed, depth and swaying acceleration during typical shallow dives made by Individual 4 in (A) weighted and (B) unweighted conditions, and deep dives made in (C) weighted and (D) unweighted conditions on July 5, 2005 (A,C) and July 6, 2005 (B,D). Vertical broken lines separate dives into three phases: descent, bottom and ascent. Swimming behavior during descent and ascent is categorized as prolonged glide (white horizontal bar), stroke-and-glide swimming (grey horizontal bar) and continuous strokes (black horizontal bar) (see 'Results' for categorization).

lipid by mass. Considering two seals with different  $P_{\text{lipid}}$  and hence  $\rho_{\text{seal}}$ , subtracting Eqn 6 for one seal from that for the other gives:

$$\Delta\rho = -\Delta P_{\text{lipid}}(\rho_{\text{lipid-free}} - \rho_{\text{lipid}}). \quad (7)$$

We used the value of  $\rho_{\text{lipid}} = 901 \text{ kg m}^{-3}$ , which was reported for humans (Moore et al., 1963) (cited by Biuw et al., 2003), and  $\rho_{\text{lipid-free}} = 1115 \text{ kg m}^{-3}$ , which we calculated from the published values of the density of various body components in humans [protein  $1340 \text{ kg m}^{-3}$ , ash  $2300 \text{ kg m}^{-3}$ , body water  $994 \text{ kg m}^{-3}$  (Moore et al., 1963) (cited by Biuw et al., 2003)] and the

proportion of each component for lipid-free-body in grey seals *Halichoerus grypus* [protein 24.3%, ash 2.8%, body water 72.9% (Reilly and Fedak, 1990)]. An increase in density ( $\Delta\rho$ ) of  $30 \text{ kg m}^{-3}$  gives  $\Delta P_{\text{lipid}}$  of  $-0.14$  according to Eqn 7, i.e. increase in  $\rho_{\text{seal}}$  by  $30 \text{ kg m}^{-3}$ , caused by the lead weight of 1.45 kg, corresponds to decrease in  $P_{\text{lipid}}$  by 14%. Pinnipeds go through dramatic seasonal changes in body lipid content, as much as 20% (Beck et al., 2000), as a result of the sometimes complete separation between feeding at sea and fasting on land while molting and lactating. We therefore believe that we could simulate such seasonal changes by attaching the lead weight,

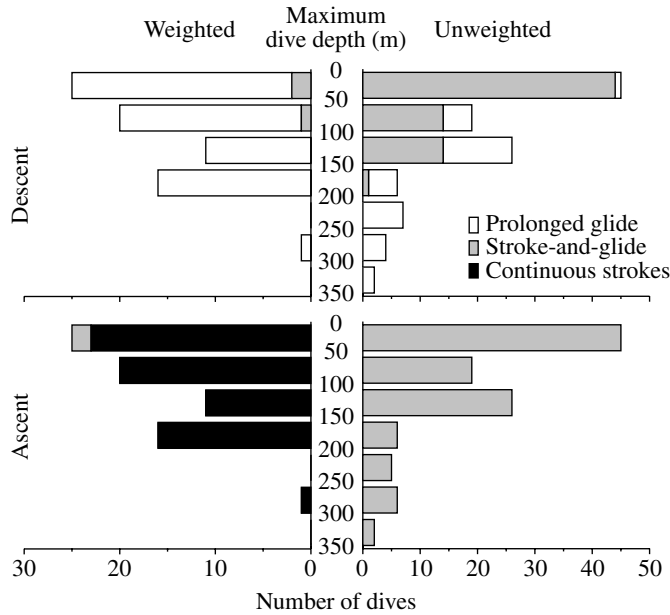


Fig. 5. Occurrence of swimming modes categorized as prolonged glide (white horizontal bar), stroke-and-glide swimming (grey horizontal bar) and continuous strokes (black horizontal bar) in relation to maximum dive depth grouped into each 50 m (see 'Results' for categorizing). Note that scales on  $x$ -axes differ between the weighted and unweighted conditions.

and suggest that seals change their stroke patterns seasonally according to their body composition.

#### Calculation of drag coefficient

We calculated drag coefficient from deceleration rates during horizontal glides (Fig. 1). This simple method has long been used in experiments with water tanks (Clark and Bemis, 1979; Bilo and Nachtigall, 1980; Videler and Kamermans, 1985; Williams and Kooyman, 1985; Feldkamp, 1987; Stelle

et al., 2000; Ribak et al., 2005), and we applied it to experiments with free-ranging animals. Miller et al. employed a different method to calculate drag coefficients of free-ranging sperm whales (Miller et al., 2004), using depth change during steep ascent glides, and therefore they needed to consider the effect of buoyancy in their calculation. The advantage of our method using horizontal glides is that the estimate of drag coefficient can be independent of that of buoyancy. Our speed sensor, which was not employed in the previous work (Miller et al., 2004), enabled us to use the method.

Drag coefficient, based on frontal area, of the seal measured in this study (0.11) is at the upper limit of the range of values previously measured in water tanks for other pinnipeds [harbor seals *Phoca vitulina*, 0.038–0.088 (Williams and Kooyman, 1985); California sea lions *Zalophus californianus*, 0.046–0.070 (Feldkamp, 1987); Steller sea lions *Eumetopias jubatus*, 0.080–0.13 (Stelle et al., 2000)]. This suggests that our logger package on the seal's back facilitated flow separation and increased drag to some extent, but not so much as to seriously affect the behavior of the seals.

#### Calculation of body density

In this study we have also demonstrated that it is possible to estimate body density from speed and pitch during prolonged glides (Figs 6, 7). Although the estimated body densities were variable among dives for both the weighted (1027–1046  $\text{kg m}^{-3}$ ,  $N=28$ ) and the unweighted (1014–1022  $\text{kg m}^{-3}$ ,  $N=25$ ) conditions, the values correspond to the theoretical difference in body density between the conditions (30  $\text{kg m}^{-3}$ ). The estimated body densities correspond to the lipid content of 32–41% and 43–47% for the weighted and unweighted conditions, respectively, according to Eqn 6. Systematic deviations of the seal data around the model density lines in Fig. 7 are perhaps caused by the fact that we did not include the effect of lift and induced drag in our model (Eqn 4). The residuals indicate that our no-lift model would underestimate body density at pitch shallower than  $\sim 45^\circ$ .

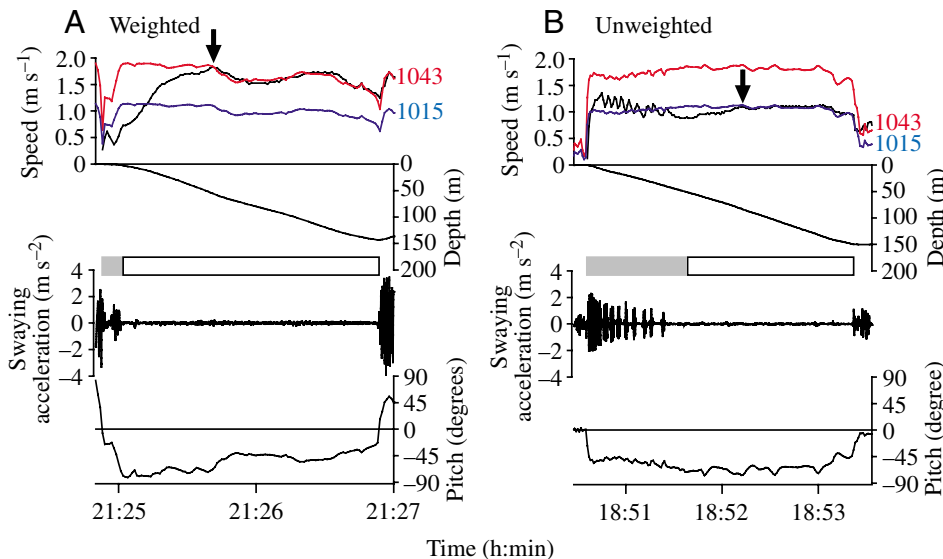


Fig. 6. Relationship between measured speed (black line) and theoretical terminal speeds, assuming a total body density of 1043  $\text{kg m}^{-3}$  (red line) and 1015  $\text{kg m}^{-3}$  (blue line), during descent phases of dives for (A) weighted (July 5, 2005) and (B) unweighted (July 7, 2005) conditions. Depth, swaying acceleration and pitch (i.e. angle between long axis of seal's body and water surface, with positive values indicating ascent and negative descent) are also shown. Swimming behavior is categorized as prolonged glide (white horizontal bar) and stroke-and-glide swimming (grey horizontal bar) (see 'Results' for categorization). Arrows indicate the first peaks of measured speed during prolonged glides.

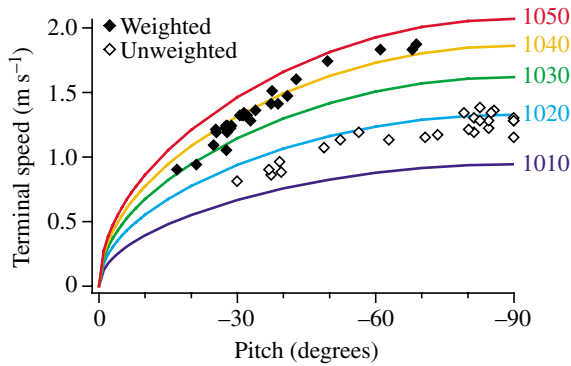


Fig. 7. Relationship between maximum speed in each prolonged glide measured at the depth of >100 m, and pitch at the moment when the speed was recorded, for weighted (solid diamonds) and unweighted (open diamonds) conditions. Pitch represents the angle between the long axis of the seal's body and the water surface, with negative values indicating descent. Theoretical terminal speeds for several body densities are shown as colored lines, with the density values in  $\text{kg m}^{-3}$  indicated by the numbers beside the lines. Strictly speaking, the theoretical lines are different between the conditions because of the different mass of the object (seal + weight=46.65 kg for the weighted condition; seal=45.2 kg for the unweighted condition; see Eqn 4) and should be shown separately. However, the difference in mass corresponds to a difference in theoretical terminal speed of only 1.6%. For clarity, we show the theoretical lines common to both conditions, based on the mean mass (45.9 kg).

More lift is needed for a buoyant animal to maintain a shallower pitch, which will correspondingly increase induced drag. Including an accurate value for induced drag would improve the estimation of body density using glides at shallow pitch.

The body density of free-ranging marine mammals was previously estimated for southern elephant seals *Mirounga leonina* using depth data during 'drift dives' (i.e. dives during which seals spend a large proportion of time drifting passively through the water column) (Biuw et al., 2003), and for sperm whales using depth and pitch during steep ascent glides (Miller et al., 2004). In the present study, we have demonstrated that measurement of terminal speed during prolonged glides is another promising approach to estimate body density and relative body composition. Furthermore, although our approach based on Newtonian mechanics is similar to those of the previous works (Biuw et al., 2003; Miller et al., 2004), we demonstrated the effect of body density on terminal glide speed by experimentally dropping the weight after a predetermined time period.

We thank P. Anoshko and E. Zemerov for their assistance with the fieldwork, M. Biuw, T. Johnson, P. Miller and A. Takahashi for helpful comments on the manuscript. This work was funded by the Japan Society for the Promotion of Science (13460082, 14405027 and 15255003), JSPS Research Fellowships for Young Scientists (Y.W.), Ministry of Education, Culture, Sports, Science and Technology, Japan

(12NP0201) and the Russian Foundation of Fundamental Science (01-04-48697).

## References

- Anon (2004). *Rika Nenpyo* (in Japanese; ed. National Astronomical Observatory). Tokyo: Maruzen.
- Baranov, E. A. (1996). A device for data retrieval and recapture of diving animals in open water. *Mar. Mamm. Sci.* **12**, 465-468.
- Beck, C. A., Bowen, W. D. and Iverson, S. J. (2000). Seasonal changes in buoyancy and diving behaviour of adult grey seals. *J. Exp. Biol.* **203**, 2323-2330.
- Bilo, D. and Nachtigall, W. (1980). A simple method to determine drag coefficients in aquatic animals. *J. Exp. Biol.* **87**, 357-359.
- Biuw, M., McConnell, B., Bradshaw, C. J. A., Burton, H. and Fedak, M. (2003). Blubber and buoyancy: monitoring the body condition of free-ranging seals using simple dive characteristics. *J. Exp. Biol.* **206**, 3405-3423.
- Burns, J. M. and Castellini, M. A. (1996). Physiological and behavioral determinants of the aerobic dive limit in Weddell seal (*Leptonychotes weddellii*) pups. *J. Comp. Physiol. B* **166**, 473-483.
- Clark, B. D. and Bemis, W. (1979). Kinematics of swimming of penguins at the Detroit zoo. *J. Zool. Lond.* **188**, 411-428.
- Davis, R. W., Fuiman, L. A., Williams, T. M. and Le Boeuf, B. J. (2001). Three-dimensional movements and swimming activity of a northern elephant seal. *Comp. Biochem. Physiol.* **129A**, 759-770.
- Falke, K., Hill, R. D., Qvist, J., Schneider, R. C., Guppy, M., Liggins, G. C., Hochachka, P. W., Elliott, R. E. and Zapol, W. M. (1985). Seal lungs collapse during free diving: evidence from arterial nitrogen tensions. *Science* **229**, 556-558.
- Feldkamp, S. D. (1987). Swimming in the California sea lion: morphometrics, drag and energetics. *J. Exp. Biol.* **131**, 117-135.
- Goldbogen, J. A., Calambokidis, J., Shadwick, R. E., Oleson, E. M., McDonald, M. A. and Hildebrand, J. A. (2006). Kinematics of foraging dives and lunge-feeding in fin whales. *J. Exp. Biol.* **209**, 1231-1244.
- Hays, G. C., Metcalfe, J. D., Walne, A. W. and Wilson, R. P. (2004). First records of flipper beat frequency during sea turtle diving. *J. Exp. Mar. Biol. Ecol.* **303**, 243-260.
- Hooker, S. K., Miller, P. J. O., Johnson, M. P., Cox, O. P. and Boyd, I. L. (2005). Ascent exhalations of Antarctic fur seals: a behavioural adaptation for breath-hold diving? *Proc. R. Soc. Lond. B Biol. Sci.* **272**, 355-363.
- Kato, A., Ropert-Coudert, Y., Grémillet, D. and Cannell, B. (2006). Locomotion and foraging strategy in foot-propelled and wing-propelled shallow-diving seabirds. *Mar. Ecol. Prog. Ser.* **308**, 293-301.
- Kooyman, G. L. (1985). Physiology without restraint in diving mammals. *Mar. Mamm. Sci.* **1**, 166-178.
- Kooyman, G. L. and Ponganis, P. J. (1998). The physiological basis of diving to depth: birds and mammals. *Annu. Rev. Physiol.* **60**, 19-32.
- Kooyman, G. L., Wahrenbrock, E. A., Castellini, M. A., Davis, R. W. and Sinnett, E. E. (1980). Aerobic and anaerobic metabolism during voluntary diving in Weddell seals: evidence for preferred pathways from blood chemistry and behavior. *J. Comp. Physiol.* **138**, 335-346.
- Kooyman, G. L., Castellini, M. A., Davis, R. W. and Maue, R. A. (1983). Aerobic dive limits in immature Weddell seals. *J. Comp. Physiol.* **151**, 171-174.
- Lovvorn, J. R., Jones, D. R. and Blake, R. W. (1991). Mechanics of underwater locomotion in diving ducks: drag, buoyancy and acceleration in a size gradient of species. *J. Exp. Biol.* **159**, 89-108.
- Lovvorn, J. R., Watanuki, Y., Kato, A., Naito, Y. and Liggins, G. A. (2004). Stroke patterns and regulation of swim speed and energy cost in free-ranging Brunnich's guillemots. *J. Exp. Biol.* **207**, 4679-4695.
- Miller, P. J. O., Johnson, M. P., Tyack, P. L. and Terray, E. A. (2004). Swimming gaits, passive drag and buoyancy of diving sperm whales *Physeter macrocephalus*. *J. Exp. Biol.* **207**, 1953-1967.
- Moore, F. D., Olsen, K. H., McMurray, J. D., Parker, H. V., Ball, M. R. and Boyden, C. M. (1963). *The Body Cell Mass and its Supporting Environment: Body Composition in Health and Disease*. Philadelphia: W. B. Saunders.
- Nowacek, D. P., Johnson, M. P., Tyack, P. L., Shorter, K. A., McLellan, W. A. and Pabst, D. A. (2001). Buoyant balaenids: the ups and downs of buoyancy in right whales. *Proc. R. Soc. Lond. B Biol. Sci.* **268**, 1811-1816.
- Ponganis, P. J., Kooyman, G. L., Baranov, E. A., Thorson, P. H. and Stewart, B. S. (1997). The aerobic submersion limit of Baikal seals, *Phoca sibirica*. *Can. J. Zool.* **75**, 1323-1327.

- Reilly, J. J. and Fedak, M. A.** (1990). Measurement of the body-composition of living gray seals by hydrogen isotope-dilution. *J. Appl. Physiol.* **69**, 885-891.
- Ribak, G., Weihs, D. and Arad, Z.** (2005). Submerged swimming of the great cormorant *Phalacrocorax carbo sinensis* is a variant of the burst-and-glide gait. *J. Exp. Biol.* **208**, 3835-3849.
- Ridgway, S. H., Scronce, B. L. and Kanwisher, J.** (1969). Respiration and deep diving in the bottlenose porpoise. *Science* **166**, 1651-1654.
- Sato, K., Naito, Y., Kato, A., Niizuma, Y., Watanuki, Y., Charrassin, J. B., Bost, C. A., Handrich, Y. and Le Maho, Y.** (2002). Buoyancy and maximal diving depth in penguins: do they control inhaling air volume? *J. Exp. Biol.* **205**, 1189-1197.
- Sato, K., Mitani, Y., Cameron, M. F., Siniff, D. B. and Naito, Y.** (2003). Factors affecting stroking patterns and body angle in diving Weddell seals under natural conditions. *J. Exp. Biol.* **206**, 1461-1470.
- Skrovan, R. C., Williams, T. M., Berry, P. S., Moore, P. W. and Davis, R. W.** (1999). The diving physiology of bottlenose dolphins (*Tursiops truncatus*) II. Biomechanics and changes in buoyancy at depth. *J. Exp. Biol.* **202**, 2479-2761.
- Stelle, L. L., Blake, R. W. and Trites, A. W.** (2000). Hydrodynamic drag in stellar sea lions (*Eumetopias jubatus*). *J. Exp. Biol.* **203**, 1915-1923.
- Stephenson, R.** (1994). Diving energetics in Lesser Scaup (*Aythya affinis*, Eyton). *J. Exp. Biol.* **190**, 155-178.
- Stephenson, R., Lovvorn, J. R., Heieis, M. R. A., Jones, D. R. and Blake, R. W.** (1989). A hydromechanical estimate of the power requirements of diving and surface swimming in Lesser Scaup (*Aythya affinis*). *J. Exp. Biol.* **147**, 507-519.
- Stewart, B. S., Petrov, E. A., Baranov, E. A., Timonin, A. and Ivanov, M.** (1996). Seasonal movements and dive patterns of juvenile Baikal seals, *Phoca sibirica*. *Mar. Mamm. Sci.* **12**, 528-542.
- Tanaka, H., Takagi, Y. and Naito, Y.** (2001). Swimming speeds and buoyancy compensation of migrating adult chum salmon *Oncorhynchus keta* revealed by speed/depth/acceleration data logger. *J. Exp. Biol.* **204**, 3895-3904.
- van Dam, R. P., Ponganis, P. J., Ponganis, K. V., Levenson, D. H. and Marshall, G.** (2002). Stroke frequencies of emperor penguins diving under sea ice. *J. Exp. Biol.* **205**, 3769-3774.
- Videler, J. and Kamermans, P.** (1985). Differences between upstroke and downstroke in swimming dolphins. *J. Exp. Biol.* **119**, 265-274.
- Vogel, S.** (1994). *Life in Moving Fluids: The Physical Biology of Flow* (2nd edn). Princeton: Princeton University Press.
- Watanabe, Y., Baranov, E. A., Sato, K., Naito, Y. and Miyazaki, N.** (2004). Foraging tactics of Baikal seals differ between day and night. *Mar. Ecol. Prog. Ser.* **279**, 283-289.
- Watanuki, Y., Niizuma, Y., Gabrielsen, G. W., Sato, K. and Naito, Y.** (2003). Stroke and glide of wing-propelled divers: deep diving seabirds adjust surge frequency to buoyancy change with depth. *Proc. R. Soc. Lond. B Biol. Sci.* **270**, 483-488.
- Watanuki, Y., Takahashi, A., Daunt, F., Wanless, S., Harris, M., Sato, K. and Naito, Y.** (2005). Regulation of stroke and glide in a foot-propelled avian diver. *J. Exp. Biol.* **208**, 2207-2216.
- Watanuki, Y., Wanless, S., Harris, M., Lovvorn, J. R., Miyazaki, M., Tanaka, H. and Sato, K.** (2006). Swim speeds and stroke patterns in wing-propelled divers: a comparison among alcids and a penguin. *J. Exp. Biol.* **209**, 1217-1230.
- Webb, P. M., Crocker, D. E., Blackwell, S. B., Costa, D. P. and Le Boeuf, B. J.** (1998). Effects of buoyancy on the diving behaviour of northern elephant seals. *J. Exp. Biol.* **201**, 2349-2358.
- Williams, T. M. and Kooyman, G. L.** (1985). Swimming performance and hydrodynamic characteristics of harbor seals (*Phoca vitulina*). *Physiol. Zool.* **58**, 576-589.
- Williams, T. M., Davis, R. W., Fuiman, L. A., Francis, J., Le Boeuf, B. J., Horning, M., Calambokidis, J. and Croll, D. A.** (2000). Sink or swim: strategies for cost-efficient diving by marine mammals. *Science* **288**, 133-136.
- Williams, T. M., Fuiman, L. A., Horning, M. and Davis, R. W.** (2004). The cost of foraging by a marine predator, the Weddell seal *Leptonychotes weddellii*: pricing by the stroke. *J. Exp. Biol.* **207**, 973-982.
- Wilson, R. P. and Liebsh, N.** (2003). Up-beat motion in swinging limbs: new insights into assessing movement in free-living aquatic vertebrates. *Mar. Biol.* **142**, 537-547.
- Yoda, K., Naito, Y., Sato, K., Takahashi, A., Nishikawa, J., Ropert-Coudert, Y., Kurita, M. and Le Maho, Y.** (2001). A new technique for monitoring the behavior of free-ranging Adélie penguins. *J. Exp. Biol.* **204**, 685-690.